ORIGINAL PAPER

Estimating the age–diameter relationship of oak species in Switzerland using nonlinear mixed-effects models

Brigitte Rohner · Harald Bugmann · Christof Bigler

Abstract Tree growth plays a key role in forest dynamics, yet little attention has been paid to quantifying tree age–diameter relationships. Predicting diameter growth of oaks is especially important due to their role in nature conservation and adaptive forest management under climate change. Thus, we (1) identified environmental variables that shape age–diameter relationships of oaks and (2) quantified the accuracy of predictions based on these variables. We determined the age–diameter relationship of 243 oaks (*Quercus* spp.) growing in Switzerland by using tree-ring samples. Nonlinear mixed-effects models based on a modified Chapman-Richards equation were fitted with environmental variables included as covariates. The fixed effects elevation, slope and water-holding capacity were most important in shaping the age–diameter relationships. Lower elevations, steeper slopes, north-facing aspects, higher water-holding capacities and moister summers resulted in larger maximum diameters. For 75 % of the oaks, age–diameter relationships predicted by the fixed effects matched fairly well the observations (root mean square error between predictions and observations <6 cm); the inclusion of random effects reduced root mean square errors for 86 % of the trees. These results suggest that water runoff plays a key role for the age–diameter relationships, accompanied by limiting temperature effects at higher elevations. The fixed effects covered variability in site quality, whereas the random effects included tree-specific deviations from expected age–diameter relationships, potentially due to neighbourhood effects such as stand density and competition.

B. Rohner · H. Bugmann · C. Bigler
Forest Ecology, Institute of Terrestrial Ecosystems, Department of Environmental Systems Science, ETH Zurich, 8092 Zurich, Switzerland

B. Rohner (✉)
Resource Analysis, Forest Resources and Management, Swiss Federal Institute for Forest, Snow and Landscape Research WSL, Zürcherstrasse 111, 8903 Birmensdorf, Switzerland
e-mail: brigitte.rohner@wsl.ch

Introduction

Tree growth is a key component of forest dynamics that has been investigated for various purposes: (1) to improve the understanding of ecological processes, e.g. growth-limiting effects of climate (Fritts 1976); (2) to quantify qualitatively well-known processes, e.g. release effects following disturbances (Black and Abrams 2003); (3) to develop models of tree growth that can be implemented in succession models (cf. Bugmann 2001); and (4) to forecast future growth, e.g. concerning expected timber yield (Hall and Clutter 2004). Thus, understanding the processes that operate on tree growth is crucial from the point of view of ecology, forest science and forest management.

Estimating tree growth has been a focus of scientific research for a long time. First attempts emerged in the form of yield tables in the early 19th century. The use of nonlinear growth equations gained popularity in the mid-20th century, when, e.g. the equation by von Bertalanffy (1957) and its

generalization by Chapman-Richards (Richards 1959) were established. Subsequently, continuous progress in statistical techniques led to the widespread use of regression methods for estimating tree growth (Tesch 1981). Recent developments have been dominated by increasing computing power, which opened the way for both simulation modelling and sophisticated empirical techniques such as mixed-effects models (Weiskittel et al. 2011).

To date, many empirical growth models have been developed to estimate the relationship between tree age and height (Lappi and Bailey 1988; Fang and Bailey 2001; Nothdurft et al. 2006), between diameter and height (Adame et al. 2008), and multivariate dependencies among dominant height, basal area and stand density (Fang et al. 2001; Hall and Clutter 2004). However, the age–diameter relationship has attracted less attention. The focus on tree height may originate from traditional yield and site considerations, because height growth is a useful proxy of site productivity (Tesch 1981). However, a tree's diameter at breast height (DBH) is an equally fundamental variable in forestry. For instance, several silvicultural characteristics including basal area or growing stock are calculated based on DBH measurements, and DBH distributions may be used to infer the successional phase of a forest (Heiri et al. 2009). In addition, growth models based on DBH may reach a higher applicability in practice since the DBH of a tree is easier to measure than its height.

The few models available for the age–DBH relationship are typically based on linear relationships (Martin-Benito et al. 2011), which restricts their applicability to the range of observed ages and diameters (cf. Pinheiro and Bates 2000). Promising nonlinear modelling approaches have attracted attention in recent times (Crecente-Campo et al. 2010; Subedi and Sharma 2011). However, empirical modelling of nonlinear growth curves—for height as well as for diameter—has often aimed at identifying the curve that best fits to the data, without considering the ecological reasons for the shape of this curve. Thus, imposing linear relationships and curve fitting without environmental covariates has limited the generality of many findings achieved so far.

A high potential for studying the development of DBH with age lies in the use of tree-ring data, since they allow for reconstructing the age–DBH relationship retrospectively at an annual resolution. While tree-ring data are ideally suited for modelling age–DBH relationships based on environmental influences, applications of such models may also involve single or repeated DBH measurements, e.g. to estimate the age of investigated trees (Rohner et al. 2013) and to predict their future growth.

Identifying environmental influences that affect the growth of oak is especially important due to their potential role in the adaptation of European forests to climate change

(e.g. Weber et al. 2007) and their high ecological value, e.g. with respect to insect and bird diversity, which has been shown to be closely related to tree size (Ranius and Jansson 2000; Caprio et al. 2009). However, the age–DBH relationship of oak has attracted only little attention so far.

Therefore, the present study aims at (1) identifying the ecological influences that underlie the age–DBH relationships of oaks across a large environmental gradient and (2) predicting the age–DBH relationship using nonlinear mixed-effects models with covariates. For these purposes, we investigated the growth curves of more than 240 oaks from 10 unmanaged forest reserves in Switzerland. The models were fitted to tree-ring data covering ages up to 280 years. We focussed on two main questions:

1. What environmental variables are important for shaping the age–DBH relationship of oak?
2. How accurate are estimates of the age–DBH relationship based on these variables?

Materials and methods

Study sites and tree species

Study sites were selected within oak forests belonging to the Swiss Forest Reserve Network, which is jointly managed by the Swiss Federal Institute for Forest, Snow and Landscape Research (WSL Birmensdorf), ETH Zurich, and the Swiss Federal Office for the Environment (FOEN; for details see Brang et al. 2011; Rohner et al. 2012; http://www.waldreservate.ch). From this network, we selected those reserves that contained a minimum proportion of *Quercus* species of 10 % in the last inventory, calculated as the importance value [(relative density + relative basal area)/2 × 100; Parker and Leopold 1983]. The composition of further tree species within the selected reserves differs strongly, ranging from mainly *Pinus sylvestris* in south-western Switzerland to mainly *Fagus sylvatica* in northern Switzerland. Additionally, only reserves with at least three inventories were considered. These criteria were met by eleven reserves, from which we excluded one located in the south-west of Switzerland (Les Follatères), because the extreme site conditions (south-facing aspect, steep slopes, shallow soils) in combination with the continental climate led to implausible model predictions for some trees (i.e. negative diameter growth). The remaining ten study sites cover more than 140 km of latitude and 230 km of longitude and represent a wide range of oak habitats varying in climatic conditions and site characteristics (Table 1).

The most frequent oak species in Switzerland are *Q. petraea, Q. robur* and *Q. pubescens,* with relative stem

Table 1 Characteristics of the study sites

Site	Coordinates (northing, easting)	Reserve area (ha)	Elevation (m a.s.l.)	Slope (°)	NSI[a]	Water-holding capacity[b]	Drought index[c] (mm)	Main soil type[d]	Main phyto-sociological association[e]	Reserve foundation (year)
Adenberg	47°36′50″, 8°33′40″	5	490–530	0–17	0.00 to 0.77	5	−4	Cambisol	*Galio odorati-Fagetum*	1970
Bannhalde	47°31′28″, 8°31′15″	2.5	425	0–14	−0.91 to 0.64	5	−5	Cambisol	*Galio odorati-Fagetum*	1972
Bois de Chênes	46°26′17″, 6°13′33″	83	500–520	0–15	−1.00 to 0.00	5	−36	Cambisol	*Carici Fagetum caricetosum montanae, Aro-Fagetum*	1969
Josenwald	47°8′5″, 9°15′19″	85	480–520	28–42	−1.00 to −0.42	1	255	Leptosol	*Teucrio-Quercetum, Asperulo taurinae-Tilietum*	1976
Krummen linden	47°33′27″, 8°20′8″	3	545–555	0	0.00	6	42	Cambisol	*Galio odorati-Fagetum luzuletosum*	1955
Langgraben	47°32′49″, 8°31′36″	4.5	420	0	0.00	4	−10	Luvisol	*Galio odorati-Fagetum luzuletosum (Galio silvatici-Carpinetum)*	1972
Pfynwald	46°17′36″, 7°33′48″	7	570–605	13–38	−1.00 to 0.97	3	−147	Regosol	*Erico-Pinetum silvestris*	1957
Strassberg	47°31′55″, 8°29′40″	6.5	465–475	6–31	−0.98 to 1.00	4	24	Cambisol	*Galio odorati-Fagetum*	1975
Vorm Stein	47°33′7″, 8°27′13″	10	475–495	0–27	−1.00 to 0.00	4	33	Luvisol	*Galio odorati-Fagetum, Pulmonario-Fagetum melittetosum*	1971
Weidwald	47°24′47″, 7°59′33″	5	610–640	6–36	−1.00 to −0.50	3	37	Leptosol	*Asperulo taurinae-Tilietum, Cardamino-Fagetum, Seslerio-Fagetum*	1963

For elevation, slope and the north–south indicator (NSI), the range represented in the tree sample is shown

[a] Calculated according to Eq. 1 (see text). An NSI of −1 represents a south-facing aspect, whereas an NSI of 1 represents a north-facing aspect. For slope = 0°, the NSI was set to zero

[b] Categories indicate the following values (in l/m²): 1: [0, 15), 2: [15, 30), 3: [30, 45), 4: [45, 60), 5: [60, 100), 6: [100, ∞)

[c] The drought index is calculated as the sum of precipitation minus potential evapotranspiration from May to July, averaged over the years 1960–2006. Bigger values of the drought index indicate moister summers

[d] Nomenclature based on the FAO system (FAO 1998)

[e] Indicated following Ellenberg and Klötzli (1972)

numbers of 61, 24 and 15 %, respectively (Swiss National Forest Inventory; Brändli 2010). We sampled and analyzed these oak species collectively (referred to as 'oak') because (1) the discrimination of the species in the field (i.e. without subsequent genetic analyses) is not reliable due to overlapping morphological attributes (Aas 1998); (2) the species also overlap in their physiological attributes (Kleinschmit and Kleinschmit 2000), and thus, we did not expect fundamentally different growth responses to environmental variables, especially not for *Q. petraea* and *Q. robur*; (3) the three species are genetically not completely isolated because all of them tend to hybridize, leading to controversies whether they are different species at all (Muir et al. 2000). As a consequence, oak species are often not discriminated in large-scale monitoring (cf. Rohner et al. 2012) and in practical applications such as Payment for Ecosystem Services schemes (e.g. Bolliger et al. 2008), i.e. efforts towards a distinct analysis may have hindered its application.

Data collection and preparation

Field methods

Field work was conducted in summer 2009 and 2010. We selected a total of 303 oaks comprising 30–31 living individuals per site, with the sample being representative of the DBH distribution recorded in the last inventory campaign. From every selected tree, one increment core was taken parallel to the contour line. Since this study was conducted within forest reserves, only one core per tree was taken to minimize the impact on the cored trees. We cored at 1.2 m above ground to avoid an impact on stem geometry at 1.3 m above ground, where the DBH is measured in the inventory campaigns.

For every cored tree, we recorded site characteristics, i.e. elevation, slope and aspect (Table 1). Slope and aspect (both in degrees) were determined based on the local topography within a radius of ca. 10 m. The azimuth of the aspect was converted into a north–south indicator (NSI) calculated as

$$\text{NSI} = \cos(\text{azimuth}/360 \times 2\pi) \qquad (1)$$

A NSI of −1 represents a south-facing aspect, whereas a NSI of 1 represents a north-facing aspect. For a slope of 0°, NSI was set to zero. NSI was included because we expected growth to be correlated with solar radiation and evapotranspiration, whereas we did not expect such a correlation for the east–west gradient.

As an indicator of soil susceptibility to drought, the water-holding capacity was determined from the Soil Suitability Map of Switzerland (Bundesamt für Raumplanung (EJPD) et al. 1980), where it is indicated in the following categories (in l/m^2): [0, 15), [15, 30), [30, 45), [45,

60), [60, 100), [100, ∞). For the statistical analysis, we transformed these categories into integers from 1 to 6 to reduce the number of coefficients to estimate and thus to improve model convergence.

Laboratory analysis

We used standard dendrochronological methods to prepare and analyze the tree cores. The surface of the cores was cut with a microtome (Gärtner and Nievergelt 2010) and prepared with chalk. The ring widths were measured using a Lintab 5 measuring system in combination with the TSAP-Win software (RINNTECH, Heidelberg, Germany). In addition to visual crossdating based on pointer years, we used the software COFECHA to quantitatively crossdate the tree-ring series at the site level (Holmes 1983).

To determine the distance and number of missing rings between the pith and the first complete ring on the core, the graphical method developed by Rozas (2003) was used. This method is based on the convergence of xylem rays and therefore allows an accurate estimation also under eccentric growth, as is often the case for oak (Rozas 2003). We excluded trees from the study (1) when crossdating failed, (2) when the distance between the pith and the first complete ring could not be determined (e.g. because the missing distance was too large), (3) when the series had both >15 % missing rings and >10 missing rings, and (4) when values were missing for site characteristics. In total, 47 trees (15.5 %) had thus to be excluded.

Data preparation

Diameter at breast height inside the bark (DBH$_{ib}$) was estimated as 2 × (cumulative sum of ring widths + estimated missing distance to the pith). The age at a tree height of 1.2 m was approximated as the sum of measured rings and the estimated number of missing rings between the pith and the first complete ring on the core. The resulting sequence of ages and corresponding DBH$_{ib}$ per tree were treated as repeated measurements in the statistical analysis.

As a proxy for the climatic conditions at the different sites, we used a drought index calculated as precipitation minus potential evapotranspiration (PET, Thornthwaite 1948; Bigler et al. 2006). The underlying data for this calculation were monthly precipitation sums and temperature means from 1960 to 2006, which were spatially interpolated to a 1-ha grid in Switzerland based on the DAYMET model (Thornton et al. 1997) by the research unit Landscape Dynamics at WSL Birmensdorf. From these data, the drought index was determined for the sites shown in Table 1. We calculated PET based on day length (estimated according to Forsythe et al. 1995) and monthly temperature means using a modified Thornthwaite (1948)

method (Willmott et al. 1985). We used the sum of drought index values from May to July because tree-ring widths showed the highest correlation with climate data from this period (Rohner 2012). For the statistical analysis, these summer drought indices were averaged over the years 1960–2006. Thus, we did not investigate the year-to-year variability of drought but focussed on general drought conditions at the included sites.

Statistical analysis

Model formulation

Nonlinear mixed-effects models with covariates were used to simultaneously model the age–DBH_{ib} relationships of the sampled oaks (Pinheiro and Bates 2000). For the nonlinear growth function, we initially considered different growth equations (e.g. von Bertalanffy, Gompertz, logistic growth; cf. Zeide 1993), but initial model fits and visual investigations revealed that the Chapman-Richards function (Richards 1959) clearly fitted the data best. Because of improved convergence, we finally used the Chapman-Richards function with an expected value parameterization for the asymptote (Fang and Bailey 2001; Hall and Clutter 2004):

$$DBH_{ib} = a \times \left(\left(1 - e^{-b \times \text{age}}\right) / \left(1 - e^{-b \times x_0}\right) \right)^c \qquad (2)$$

where the parameter a represents the estimated DBH_{ib} at age x_0, b is a slope parameter, and c defines the type of the curve (i.e. presence of an inflection point). The value x_0 is an arbitrary reference age that may be fixed at any positive value (Fang and Bailey 2001). In yield modelling where tree height is modelled in relation to age, x_0 is usually taken as the site index reference age since parameter a then corresponds to the site index. However, in the present study, we focussed on general features of the age–diameter relationship, among others the potential maximum diameters. The value x_0 was therefore set to 1,200 years, the maximum age reported for *Q. robur* (Godet 1986). The slope parameter b defines how fast a tree approaches its asymptotic diameter (DBH_{ib_asym}), which can be calculated as (Fang and Bailey 2001):

$$DBH_{ib\_asym} = a / \left(1 - e^{-b \times x_0}\right)^c \qquad (3)$$

For all three parameters (a, b, c), we estimated fixed effects, whereas an additional random intercept for the parameter a was predicted per tree. The decision whether to include random effects for the particular parameters was based on the ratio between the standard deviation of the random effect and the corresponding parameter estimates in the initial model fits (Pinheiro and Bates 2000). This ratio was relatively high for a (0.3), but very low for b and c (both $<10^{-7}$). The fixed effects for a and b were

modelled as linear combinations of various covariates (Pinheiro and Bates 2000). Thus, the vectors containing all tree-specific estimates of a and b were composed as follows:

$$\vec{a} = X \times \vec{\alpha} + \vec{r} \qquad (4)$$

$$\vec{b} = Y \times \vec{\beta} \qquad (5)$$

where X and Y are matrices containing the covariates for all trees, $\vec{\alpha}$ and $\vec{\beta}$ are vectors representing the coefficients of the covariates, and $\vec{r}$ indicates the vector of the random intercepts for parameter a. No covariates for explaining parameter c were considered; although we expected the temporal development of competition to have the highest influence on c, we lacked the necessary data to reconstruct competition along time.

A set of 100 competing models was formulated with varying combinations of covariates included in X (Eq. 4) and Y (Eq. 5); a complete list of all considered models is shown in the Online Resource 1. All possible combinations among topographical variables (i.e. elevation, slope and the NSI), water-holding capacity and drought index and additional combinations with the interaction between water-holding capacity and drought index were considered. We included the interaction between water-holding capacity and drought index because we expected a stronger effect of the drought index at sites with a low water-holding capacity, and vice versa. No other interactions were included because no intensifying effect was expected among topographical variables and water-holding capacity, and the interaction between topographical variables and the drought index would have entailed too many additional parameters to estimate, thus leading to convergence problems.

We randomly selected a total of 200 trees with 20 trees per study site to fit each of the 100 models, whereas the remaining 43 trees were subsequently used as independent data for model evaluation (13 trees had to be excluded due to convergence problems caused by almost linear growth curves). In the fitting procedure, we incorporated a first-order autoregressive process to model the temporal autocorrelation of the residuals (Pinheiro and Bates 2000). In addition, all covariates were centred and scaled to avoid convergence problems and to achieve comparability among parameter estimates (means and standard deviations used for scaling and centering are shown in the Online Resource 2). All pairwise Pearson correlations between the covariates were $<|0.6|$, with the only exception of slope and water-holding capacity ($r = -0.8$).

Model evaluation and averaging

We evaluated the models following an information-theoretic approach based on the Akaike Information Criterion

(AIC, Burnham and Anderson 2002). Thus, we ranked all models according to their Akaike weights w_i, which are defined as

$$w_i = e^{-\frac{1}{2}\Delta_i} \bigg/ \sum_{i=1}^{100} e^{-\frac{1}{2}\Delta_i} \qquad (6)$$

with Δ_i being the difference in AIC between model i and the model with the lowest AIC (Burnham and Anderson 2002). The Akaike weight of a model may be interpreted as the probability that this model best describes the data at hand among the 100 models that we fitted (Johnson and Omland 2004).

Since several models reached a notable Akaike weight, multi-model inference was performed. This approach allowed to take into account the considerable uncertainty in model selection, which were completely ignored by using solely the 'best' model for inference and prediction (Burnham and Anderson 2002; Johnson and Omland 2004). In cases where no single model is clearly superior (e.g. w_i >0.9, cf. Burnham and Anderson 2002) and quantitative prediction is the main goal, multi-model inference is particularly recommended to achieve more robust predictions (Burnham and Anderson 2002; Johnson and Omland 2004). In addition, multi-model inference may be beneficial for discussing the relative importance of explanatory variables, because it allows for more flexible interpretations than 'important versus not important'. Thus, we averaged the model-specific coefficient vectors $\vec{\alpha}_i$ over all models based on a weighting scheme representing the w_is, according to

$$\vec{\alpha}_{\text{averaged}} = \sum_{i=1}^{100} w_i \times \vec{\alpha}_i \qquad (7)$$

and analogously for $\vec{\beta}_{\text{averaged}}$. When a covariate was not present in a model, its coefficient was set to zero (Burnham and Anderson 2002; Johnson and Omland 2004). The corresponding standard errors were averaged from the model-specific standard error vectors $\vec{se}_{\alpha,i}$ as

$$\vec{se}_{\alpha,\text{averaged}} = \sum_{i=1}^{100} \left(w_i \times \sqrt{\vec{se}_{\alpha,i}^2 + \left(\vec{\alpha}_i - \vec{\alpha}_{\text{averaged}}\right)^2} \right) \qquad (8)$$

and analogously for $\vec{se}_{\beta,\text{averaged}}$. Only those models were considered in which the particular covariate was present, because setting the standard error to zero in models in which the corresponding covariate does not occur would bias the averaged standard error towards zero. Therefore, we linearly adjusted the w_is that they sum up to 100 % when considering only those models in which the respective covariate was present. No p-values could be specified for the averaged coefficients; however, since the coefficients are assumed to be normally distributed, the interval $\pm 1.96 \times se_{\text{averaged}}$ around the coefficients can be used as

an indicator of the significance. The goodness of the averaged model fit was quantified based on the root mean square error (RMSE) between the observed and predicted DBH_{ib}.

Model validation

A sensitivity analysis was performed to investigate the modelled effects of the explanatory variables on the age–DBH_{ib} curves. For this purpose, one explanatory variable at a time was varied, while all the others were fixed at their respective mean. The corresponding age–DBH_{ib} curves predicted by the averaged model were examined with regard to plausibility.

The generality of the averaged model was evaluated by applying it to the 43 validation trees, which had not been used for the model fitting procedure. For these validation trees, the age–DBH_{ib} relationship was predicted based on the fixed effects of the averaged model only. Random effects could have been calibrated for the validation trees only if at least one age–DBH_{ib} observation per validation tree was assumed to be known (cf. Fang and Bailey 2001; Nothdurft et al. 2006). We refrained from this assumption since tree age is often unknown for oaks. Again, we calculated the RMSE between the observed and predicted DBH_{ib} to quantify the goodness of the prediction.

All statistical analyses were performed using the packages *nlstools* (Baty and Delignette-Muller 2011) and *nlme* (Pinheiro et al. 2011) in *R*, a language and environment for statistical computing (version 2.11.1, *R* Development Core Team 2010).

Results

Description of age and diameter data

Summary statistics of tree age and DBH_{ib} are shown in Table 2 for both the modelling and the validation sample. Ages at sampling height ranged from 21 to 282 years with the corresponding DBH_{ib} varying between 3.5 and 77.9 cm. Although mean ages and DBH_{ib} were slightly higher in the validation sample than in the modelling sample, the represented ranges of ages and DBH_{ib} were similar for both samples (Table 2).

Model evaluation and averaging

Nine models reached Akaike weights between 0.03 and 62 %, and the remaining 91 models had Akaike weights <0.01 % (Table 3, Online Resource 1). For describing the parameters a and b, the same three covariate combinations were present in the models with Akaike weights >0.01 %,

Table 2 Summary statistics of ages and diameters inside bark (DBH$_{ib}$) of the included oaks

	Age (years)		DBH$_{ib}$ (cm)	
	Modelling sample	Validation sample	Modelling sample	Validation sample
Mean	108	128	25.8	30.1
Standard deviation	53	68	14.3	15.6
Minimum	21	27	3.5	5.9
Maximum	282	273	77.9	76.0

Values refer to the year 2008. The modelling sample comprises 200 oaks (20 oaks randomly selected per reserve), whereas the validation sample comprises the remaining 43 oaks

Table 3 Models with Akaike weights >0.01 %

Model number	Parameter a[a]				Parameter b[a]				Akaike weight (%)
	Topography[b]	Water-holding capacity	Drought index	Interaction[c]	Topography[b]	Water-holding capacity	Drought index	Interaction[c]	
50	×	×			×	×			0.03
53	×	×	×		×	×			0.59
55	×	×	×	×	×	×			0.60
77	×	×			×	×	×		4.06
80	×	×	×		×	×	×		1.23
82	×	×	×	×	×	×	×		1.43
95	×	×			×	×	×	×	62.20
98	×	×	×		×	×	×	×	22.27
100	×	×	×	×	×	×	×	×	7.60

A complete list of all considered models is shown in the Online Resource 1.

[a] The parameters a (Eq. 4) and b (Eq. 5) are from the modified Chapman-Richards growth equation (Eq. 2; Richards 1959; Fang and Bailey 2001; Hall and Clutter 2004)

[b] Topography includes elevation, aspect and the north–south indicator

[c] Interaction between water-holding capacity and drought index

i.e. (1) topography and water-holding capacity; (2) topography, water-holding capacity and drought index; and (3) topography, water-holding capacity, drought index and the interaction between the water-holding capacity and the drought index. Thus, topography and water-holding capacity were present for both parameters a and b in every model with Akaike weights >0.01 %.

Model averaging resulted in the coefficients and standard errors shown in Table 4. Parameter a was strongly negatively correlated with elevation and strongly positively correlated with slope and water-holding capacity. In addition, the NSI and the drought index showed a weakly positive correlation with a, but the interval $\pm 1.96 \times se_{averaged}$ around the coefficients included zero. By far the weakest correlation with parameter a was found for the interaction between water-holding capacity and the drought index. For parameter b, all coefficients showed opposite algebraic signs compared to parameter a, with the intercept being the only exception (Table 4). In fact, the estimates of the parameters a and b were strongly negatively correlated (Pearson correlation coefficient = −0.94, see Online Resource 3).

The averaged model predicted values of the parameter a between 14.3 and 109.1 for the trees used in the model selection procedure (Online Resource 3), which corresponds to the expected DBH$_{ib}$ when oaks reach an age of 1,200 years. For parameter b, values between 9.4×10^{-4} and 8.1×10^{-3} were predicted. DBH$_{ib\_asym}$ resulting from these parameter estimates (Eq. 3) covered a range between 14.3 and 148.3 cm, with 50 % of the trees reaching a predicted DBH$_{ib\_asym}$ between 60 cm and 80 cm (Fig. 1).

For most of the trees included in the model fitting procedure, the age–DBH$_{ib}$ curves predicted by the fixed effects of the averaged model were fairly close to the observed curves (Fig. 2, for predictions of all trees see Online Resource 4). The RMSE was <3 cm for 47 % of the trees, and for 80 % of the trees <6 cm. The inclusion of a random term reduced the RMSE for 86 % of the trees (Fig. 2). This reduction was generally larger for trees whose predictions based on the fixed effects had a high RMSE. Those 14 % of the trees for which the inclusion of a random term increased the RMSE had an RMSE <6 cm based on the fixed effects only (Fig. 2).

Table 4 Coefficients ± standard errors of the averaged model

Parameters	Intercept	Topography		NSI[b]	Water-holding capacity	Drought index	Interaction[c]	Random intercept (standard deviation)
		Elevation	Slope					
a[a]	67.52 ± 2.38	−19.31 ± 2.15	17.95 ± 3.20	2.36 ± 3.26	24.49 ± 3.12	0.83 ± 3.10	−0.083 ± 2.40	19.23
b[a]	0.0042 ± 0.00021	0.0013 ± 0.00012	−0.0015 ± 0.00016	−0.00034 ± 0.00015	−0.0017 ± 0.00021	−6.9e-05 ± 0.00024	−0.00022 ± 0.00011	
c[a]	0.86 ± 0.0070							

[a] The parameters are from the modified Chapman-Richards growth equation (Eq. 2; Richards 1959; Fang and Bailey 2001; Hall and Clutter 2004)

[b] North–south indicator; calculated according to Eq. 1 (see text)

[c] Interaction between water-holding capacity and drought index
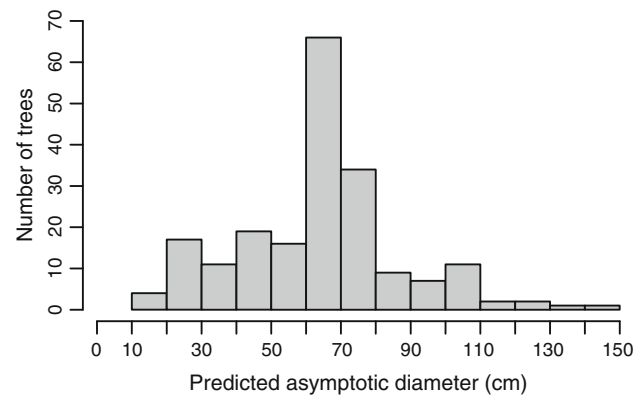
Fig. 1 Predicted asymptotic diameters. The asymptotic diameter of every tree used for the model fitting procedure was calculated from the parameter estimates as $a/\left(1 - e^{-b \times x_0}\right)^c$, where x_0 was set to 1,200 years

Model validation

The sensitivity analysis generally resulted in plausible growth curves and further emphasized differing effect sizes of the individual explanatory variables (Fig. 3). The predicted age–DBH$_{ib}$ curves were most sensitive to varying elevations and water-holding capacities (Fig. 3a, c) and nearly insensitive to varying drought indicators and NSI (Fig. 3d, e). In general, age–DBH$_{ib}$ curves were predicted to increase faster and to level off later at lower elevations, steeper slopes and on soils with higher water-holding capacities. However, at sites with slopes $\geq 30°$ and water-holding capacities ≥ 100 l/m^2, these trends changed such that predicted growth curves increased slower and were less curved during the first hundreds of years (Fig. 3b, c).

The application of the averaged model (Table 4) to the validation trees revealed a similar distribution of the RMSE as for the trees used for model fitting (Fig. 4, model predictions for all validation trees are shown in the Online Resource 5). Again, almost half of the trees (49 %) had an RMSE <3 cm between the observed and predicted DBH$_{ib}$, and a further 26 % had an RMSE <6 cm (Fig. 4). For some trees, the predictions fitted the observations fairly well until a certain age was reached, but abrupt growth changes subsequently led to an increasing divergence between the two curves (e.g. Fig. 4c, d).

Discussion

Parameter estimation of the Chapman-Richards function

The use of nonlinear mixed-effects models for describing the age–diameter relationships of oaks in Switzerland
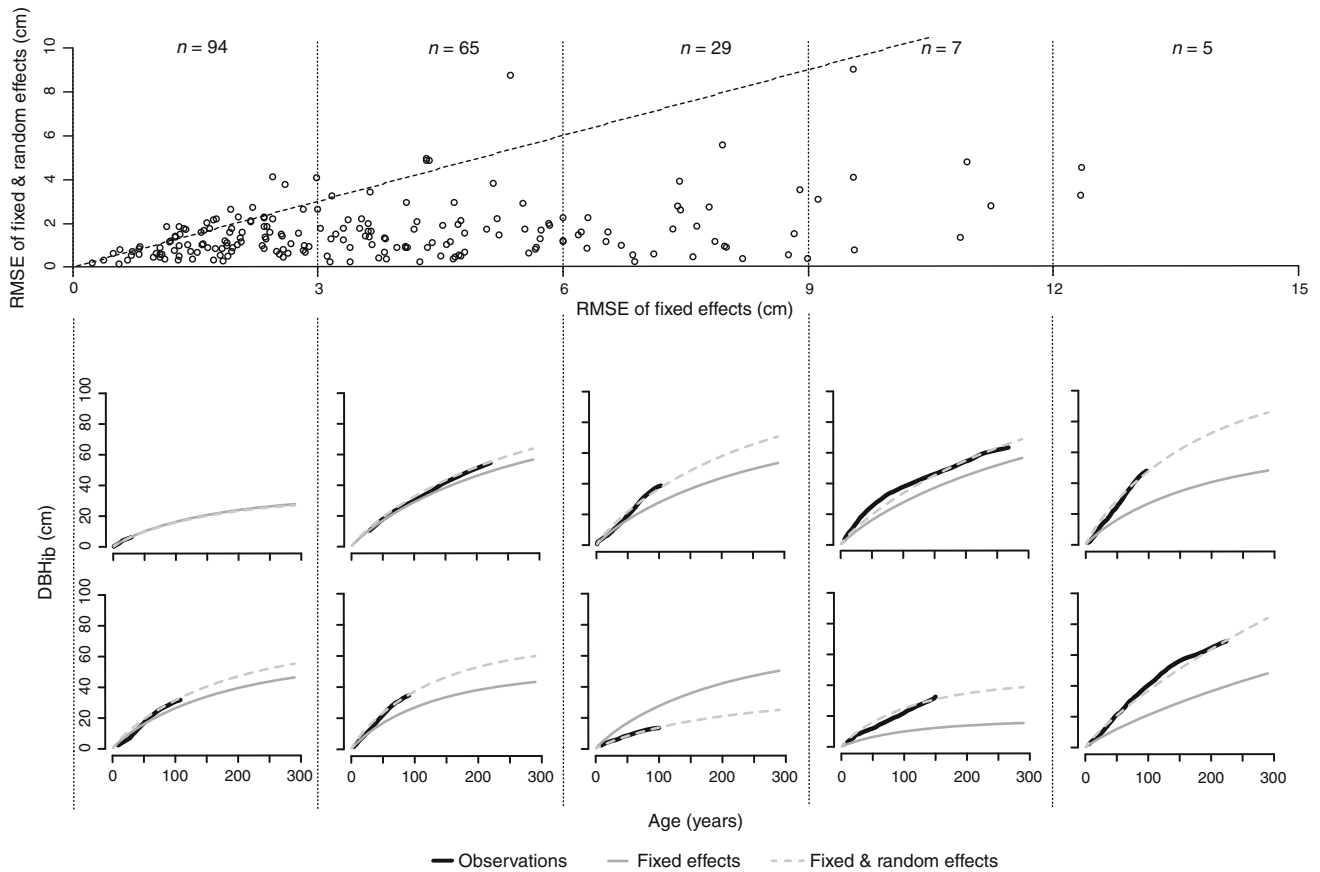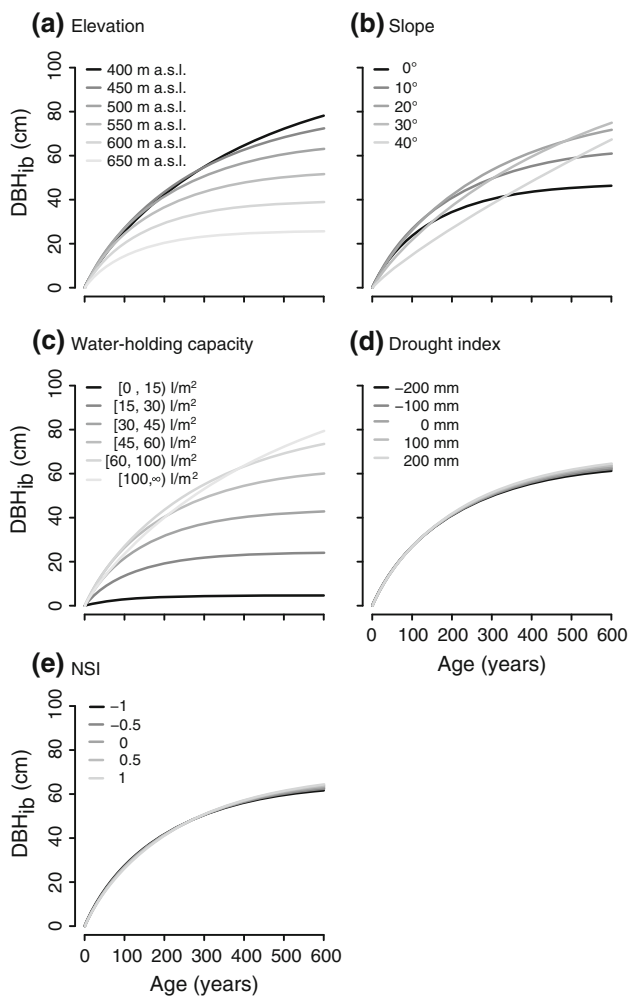
Fig. 2 Accuracy of the averaged model (see Table 4). In the *upper part*, the root mean square error (RMSE) of the model fit based on the fixed effects is plotted against the RMSE of the model fit including both fixed and random effects. For all points below the dashed line, the inclusion of the random effect reduced the RMSE. Five classes were formed according to the RMSE based on the fixed effects (RMSE 0–3, 3–6, 6–9, 9–12, >12 cm; indicated by vertical dotted lines), for which *n* indicates the number of trees in the corresponding class. Three trees outside the range of the graph are not shown (RMSE of the fixed effects: 16.2, 19.3, 21.1 cm). In the *lower part*, the model predictions are shown for the trees with the lowest (above) and highest (below) RMSE of the corresponding class, respectively. DBH$_{ib}$ indicates diameter inside the bark at a height of 1.2 m. Predictions for all trees used in the model fitting procedure are shown in the Online Resource 4

resulted in accurate predictions and entailed several methodological advantages compared to alternative modelling approaches. First, the accuracy of the predictions is likely to result from the relatively flexible nonlinear Chapman-Richards growth equation. Second, this equation allows for projections outside the range of available data, e.g. for higher ages. Such projections are more reliable than those from *linear* mixed-effects models, e.g. polynomial models (Pinheiro and Bates 2000). Third, the Chapman-Richards growth equation has a biologically motivated background (Zeide 1993), which implies that estimating its parameters is equivalent to quantifying the ecological processes underlying the function (e.g. the growth constraint reflected in parameter *a*). Lastly, the inclusion of covariates allows for quantifying ecological influences on these processes.

The parameter *c* was estimated to be <1, suggesting that the age–diameter relationship was most appropriately modelled without an inflection point. This contrasts von Bertalanffy's (1957) growth equation, where *c* equals 3 based on theoretical considerations. However, these considerations were mainly geared towards animal rather than plant growth. The shape of the growth curves of the individual trees likely depends on the competitive situation within their neighbourhood, with strong competition leading to flat sections in the growth curve and release from competition to steep parts of the curve. The estimation of a fixed *c* value for all trees in the sample neglects individual variations in the form of the growth curves that are possibly induced by suppression and release phenomena; therefore, this is likely to entail an increased RMSE for at least some trees in the sample. It would be possible to adjust the parameter *c* individually across time if the competitive situation of every tree could be reconstructed (cf. Weber et al. 2008), but due to the decay of dead trees this is feasible only for the past 10–20 years. Such an endeavour

Fig. 3 Sensitivity analysis of the averaged model (see Table 4). Age–DBH$_{ib}$ curves were predicted by varying the **a** elevation, **b** slope, **c** water-holding capacity, **d** drought index, and **e** north–south indicator (NSI) while the other explanatory variables were fixed at their mean (mean values of the explanatory variables are shown in the Online Resource 2). *DBH$_{ib}$* indicates the diameter inside the bark at a height of 1.2 m

is not feasible in forest reserves because a dendrochronological analysis of all trees in the plot would be required.

The estimated values of DBH$_{ib\_asym}$ and the parameter *a* (DBH$_{ib}$ at the age of 1,200 years) seem to be rather low. However, representative reference values are rare and often speculative, since most trees are cut or die prior to reaching such high ages. Maximum diameters reported in the literature range between 250 and 300 cm for *Q. petraea*, 200–380 cm for *Q. robur*, and around 90 cm for *Q. pubescens* (cf. Bugmann 1994) and thus are considerably higher than those predicted by the averaged model, especially if we assume that *Q. pubescens* represents the lowest estimated DBH$_{ib\_asym}$. Furthermore, *Q. robur* trees with an age of only 250–450 years have been recorded with DBHs similar to or even exceeding the DBH$_{ib\_asym}$ estimated in

the present study (Rozas 2005). An explanation for this discrepancy may be that reported maximum DBHs are likely to originate from exceptionally vigorous sites, whereas many dry sites with shallow soils were included in the present study. A difference of a few centimetres between DBH and DBH$_{ib}$ due to the bark (bark thickness varied between 0.2 and 2.5 cm; B. Rohner, unpublished) provides another explanation. And finally, a further reason for the underestimation of the diameters in our model is the assumption of concentric growth, which is reflected in the fact that only one core per tree was sampled and the tree-ring widths were measured perpendicular to the ring boundaries. This assumption has been shown to be often violated for oaks (Rozas 2003) and to potentially bias long-term increment projections for both coniferous and deciduous tree species (Russell et al. 2011). Hence, for a sound comparison with DBH values measured by calliper, corrections of the DBH$_{ib}$ related to bark thickness and eccentric growth would be necessary. However, when discussing these possible reasons for the comparably low values of estimated DBH$_{ib\_asym}$, it should be kept in mind that ages represented in our study covered the range between 21 and 282 years, and therefore, estimated DBH$_{ib\_asym}$ reflect predictions far outside the range of represented data.

The estimated values of the slope parameter *b* need to be interpreted in combination with the corresponding values of *a* because they are strongly negatively correlated. This correlation likely results from annual diameter growth being restricted to a biologically plausible range. For example, if we compare two trees with an expected DBH$_{ib\_asym}$ of 15 versus 150 cm, the same value of *b* for these two trees would imply the same time available for approaching DBH$_{ib\_asym}$—this would likely entail implausible annual growth rates for either of them (for a visualization see Online Resource 6). This holds particularly true for oak, because a minimum tree-ring width is produced in most years (Rozas 2003). Accordingly, a lower value of *b* in combination with a higher value of *a* may still represent higher annual growth over a certain time span (see Online Resource 6). Hence, the slope parameter *b* does not have a consistent biological interpretation (cf. Richards 1959), and this is why we hereafter focus on parameter *a*.

Environmental variables shaping the age–diameter relationship

The estimated coefficients of several covariates for *a* as well as the sensitivity analysis indicate that, although water stress seems to be a key process limiting the age–DBH$_{ib}$ relationship of oak, the amount of water being potentially present at a particular site is less important than the capability of retaining this amount. For instance, the
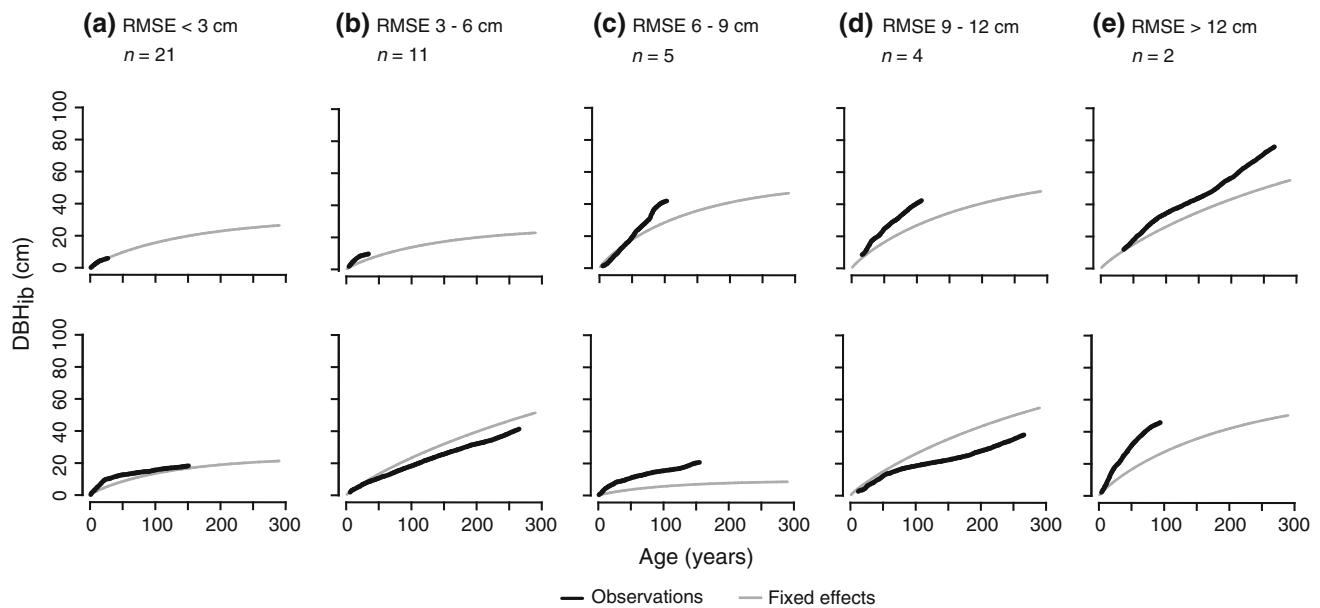
Fig. 4 Application of the averaged model (see Table 4) to the validation trees. The trees of the validation sample were grouped according to the root mean square error (RMSE) the same way as the trees used for model fitting (**a–e**, see Fig. 2). For every group, n indicates the number of trees, and the model prediction is shown for the tree with the lowest (*above*) and the highest (*below*) RMSE. DBH_{ib} indicates the diameter at 1.2 m inside the bark. Predictions for all validation trees are shown in the Online Resource 5

highest correlation was found between parameter a and the water-holding capacity, representing increasing DBH_{ib} at 1,200 years with increasing water-holding capacity. A likely explanation for this correlation is that trees on soils with a high water-holding capacity experience prolonged water supply during dry periods, whereas tree growth on soils with a low water-holding capacity may already be limited by drought early on in rainless periods. The water-holding capacity has been shown to be important in the age–height relationship of various tree species in Europe, including *Q. petraea* (e.g. Piedallu et al. 2011), whereas influences on diameter growth have been found mainly in the context of annual increments (Weber et al. 2007). We are not aware of quantitative studies on possibly limiting effects on maximum tree diameter. The impact of the water balance on maximum diameter is further corroborated by the positive coefficient of the NSI, which indicates a higher DBH_{ib} at 1,200 years on north-facing aspects, where lower evapotranspiration is expected.

Although the positive correlation between parameter a and the drought index is weak, this relationship further supports the conclusion that water stress is limiting the maximum diameter of oak. The influence of year-to-year drought variability on diameter growth was not investigated here since parameters a and b are characteristics of the growth curves as a whole; they do not vary over time. Consequently, potential effects on short-term variations in the steepness of the growth curves could not be analyzed

within the scope of the present study. The typical approach to quantify effects of time-varying climate variables on tree growth is based on correlation or response functions that require standardized growth indices (Fritts 1976).

The comparably high negative correlation between elevation and DBH_{ib} at 1,200 years may be indicative of frost conditions. Reduced tree dimension with increasing elevation due to temperature limitation is a well-known process that usually occurs at the upper end of a tree species' distribution range. The upper elevation limit of oaks in Central Europe is located at around 1,000 m a.s.l. (Ellenberg and Leuschner 2010). The elevation gradient represented in our study thus covers a considerable amount of this distribution range. Lower temperatures at higher elevations may increase the risk of frost damage, for which oak is known to be susceptible (Ellenberg and Leuschner 2010). Furthermore, in the European Alps the length of the growing season decreases by 7 days per 100 m of elevation gain (Gensler 1946). At higher elevations, these well-known effects of reduced temperature are likely to limit the maximum diameter of oak.

The positive effect of slope on parameter a indicates an increased DBH_{ib} of 1,200-year-old oaks on steeper slopes. This is rather unexpected as steep slopes are commonly associated with adverse growing conditions (e.g. Costa et al. 2008), e.g. due to high runoff and shallow soils. However, a geometrical effect may have caused increased asymptotic diameter values: the horizontal projection of a

tree crown to the ground represents a larger area on steep compared to flat terrain. As a consequence, the root zone—and thus accessible water and nutrients—per tree may be larger on steeper slopes if identical soil depth is assumed. Analogously, the available canopy space per tree may be larger on steeper slopes. However, such potential benefits have not been documented so far. Thus, the possibility that the positive coefficient for slope could be an artefact caused by the comparably high correlation with water-holding capacity cannot be ruled out. Furthermore, the sensitivity analysis revealed that diameter growth may be reduced at very steep slopes for the first hundreds of years—despite the positive correlation between slope and parameter a.

It is worth emphasizing that our interpretations regarding the importance of water stress do not contradict the drought tolerance ascribed to oak. In fact, $Q.$ $robur$ and $Q.$ $petraea$ are able to grow under fairly dry conditions, although their optimum growth range lies in moist conditions, where they are usually suffering from high competition by more shade-tolerant species such as European beech ($F.$ $sylvatica$; Ellenberg and Leuschner 2010). From this perspective, it is not surprising that reduced parameter values for a and associated DBH_{ib_asym} are predicted under drier conditions. Our model does not investigate $whether$ oaks are able to grow, but it quantifies how they grow under specific conditions along an environmental gradient.

Accuracy and applicability of the age–diameter model

Although the present study generated an empirical growth model with possible applicability in a wide range of Central European oak forests, the simultaneous consideration of a south-facing $Q.$ $pubescens$ forest that is characterized by shallow soils located in the comparably dry Valais (Les Follatères) did not produce plausible results. This is likely due to the fact that Les Follatères covers the upper end of the elevation gradient (up to 870 m a.s.l.) as well as the lower end of the NSI (−1 to 0.71). Furthermore, Les Follatères has the second lowest water-holding capacity among all study sites (category 2, i.e. [15, 30) l/m^2), only undermatched by Josenwald, where the drought index indicates moister summer conditions, though (precipitation−PET from May to July = −9 mm at Les Follatères). Oaks from Les Follatères therefore struggle with adverse conditions, comparable to those in the Mediterranean area. The inability of the model to cope with such conditions indicates that its applicability to oaks from southern Europe is highly restricted.

The fixed effects of the averaged model reflected well the general variability in the age–diameter curves for the majority of the oaks in our sample. Since a broad range of growth-relevant site characteristics were represented by the

fixed effects, they are likely to have captured site quality fairly well. The similar RMSE distributions of the model fitting and the validation sample indicate that predictions from the averaged model are robust within the range of incorporated site characteristics. However, under specific site conditions, there is substantial variability in the age–diameter curves that cannot be explained by the fixed effects alone.

The inclusion of an additional random effect led to considerable improvement in the predictions for trees whose age–diameter relationship was captured only poorly by the fixed effects. In general, estimates based on both fixed and random effects fitted the observations very accurately. Similar improvements by adding random effects were found in a variety of empirical growth-modelling studies based on linear (Martin-Benito et al. 2011) and nonlinear relationships (Nothdurft et al. 2006; Adame et al. 2008; Subedi and Sharma 2011). However, tree-specific random effects are predicted during the fitting procedure and are therefore not directly transferable to independent trees. Although it is possible to calibrate random effects if at least one observation per independent tree is known (Fang and Bailey 2001; Nothdurft et al. 2006), this condition is often not met since tree age remains unknown in many ecological applications. This is particularly true for oaks, which have often been left over from former coppice-with-standards management. Nevertheless, estimating future growth of such oaks becomes increasingly important in nature conservation projects, where compensation payments to forest owners have to be determined, but invasive methods for age determination are not allowed or too expensive. Our findings may thus be applied in two different contexts: (1) in the case of oaks for which only site information is available, the age–diameter relationship may be predicted based on the fixed effects alone; (2) in the case of oaks for which at least one additional age–diameter observation is available, random effects may be calibrated (cf. Fang and Bailey 2001; Nothdurft et al. 2006) to base the predictions on both fixed and random effects.

The random effects in the present study accounted for individual deviations from expected site-specific age–diameter relationships that cannot be explained by the fixed effects. A considerable part of these deviations probably reflects variability in the competitive situation among individual trees. Growth effects caused by competition have not been included in the fixed effects because their reconstruction over longer time spans is a very cumbersome task (cf. Weber et al. 2008). However, efforts to solve this issue would be desirable, since the inclusion of information on the temporal development of the competitive situation in the fixed effects would be highly likely to improve the predictions based on the fixed effects alone.

Conclusions

Nonlinear mixed-effects models with covariates are a promising tool to model tree growth and specifically the age–diameter relationship of oak trees, because they allow for the identification of drivers acting on tree growth as well as for the prediction of tree growth. The model that we derived indicates that water runoff in combination with frost damage and a restricted length of the growing season towards the upper elevation limit are crucial site characteristics shaping the age–diameter relationship of oak. Predictions based on the fixed effects of the model are fairly accurate, and the accuracy can be increased considerably by including an additional tree-specific random effect. This random effect accounts for potential influences that were not measured such as stand density and competition. The present findings can be used in future attempts to predict oak growth in Central Europe, be it for purposes of biodiversity conservation or for adaptive management strategies under climate change.

References

Aas G (1998) Morphologische und ökologische Variation mitteleuropäischer *Quercus*-Arten: Ein Beitrag zum Verständnis der Biodiversität. Libri botanici 19. IHW-Verlag, Eching bei München

Adame P, del Río M, Cañellas I (2008) A mixed nonlinear height-diameter model for pyrenean oak (*Quercus pyrenaica* Willd.). For Ecol Manage 256:88–98

Baty F, Delignette-Muller ML (2011) nlstools: tools for nonlinear regression diagnostics. R package version 0.0-11

Bigler C, Bräker OU, Bugmann H, Dobbertin M, Rigling A (2006) Drought as an inciting mortality factor in Scots pine stands of the Valais, Switzerland. Ecosyst 9:330–343

Black BA, Abrams MD (2003) Use of boundary-line growth patterns as a basis for dendroecological release criteria. Ecol Appl 13:1733–1749

Bolliger M, Schnidrig R, Stadler B (2008) Fachspezifische Erläuterungen zur Programmvereinbarung im Bereich Waldbiodiversität. In: Handbuch NFA im Umweltbereich. Bundesamt für Umwelt BAFU, Bern

Brändli, U.-B. (ed) (2010) Schweizerisches Landesforstinventar. Ergebnisse der dritten Erhebung 2004–2006. Eidgenössische Forschungsanstalt für Wald, Schnee und Landschaft WSL, Birmensdorf; Bundesamt für Umwelt BAFU, Bern

Brang P, Heiri C, Bugmann H (2011) Waldreservate. 50 Jahre natürliche Waldentwicklung in der Schweiz. Haupt, Bern

Bugmann HKM (1994) On the ecology of mountainous forests in a changing climate: a simulation study. Dissertation, ETH Zurich, Zurich

Bugmann H (2001) A review of forest gap models. Clim Change 51:259–305

Bundesamt für Raumplanung (EJPD), Bundesamt für Landwirtschaft (EVD), Bundesamt für Forstwesen (EDI) (1980) Bodeneignungskarte der Schweiz. Grundlagen für die Raumplanung. Eidgenössische Drucksachen- und Materialzentrale, Bern

Burnham KP, Anderson DR (2002) Model selection and multimodel inference: a practical information-theoretic approach, 2nd edn. Springer, New York

Caprio E, Ellena I, Rolando A (2009) Native oak retention as a key factor for the conservation of winter bird diversity in managed deciduous forests in northern Italy. Landsc Ecol 24:65–76

Costa A, Madeira M, Oliveira ÂC (2008) The relationship between cork oak growth patterns and soil, slope and drainage in a cork oak woodland in Southern Portugal. For Ecol Manage 255:1525–1535

Crecente-Campo F, Soares P, Tomé M, Diéguez-Aranda U (2010) Modelling annual individual-tree growth and mortality of Scots pine with data obtained at irregular measurement intervals and containing missing observations. For Ecol Manage 260: 1965–1974

Ellenberg H, Klötzli F (1972) Waldgesellschaften und Waldstandorte der Schweiz. Mitteilungen der Schweizerischen Anstalt für das Forstliche Versuchswesen 48:589–930

Ellenberg H, Leuschner C (2010) Vegetation Mitteleuropas mit den Alpen, 6th edn. Ulmer, Stuttgart

Fang Z, Bailey RL (2001) Nonlinear mixed effects modeling for slash pine dominant height growth following intensive silvicultural treatments. For Sci 47:287–300

Fang Z, Bailey RL, Shiver BD (2001) A multivariate simultaneous prediction system for stand growth and yield with fixed and random effects. For Sci 47:550–562

FAO (1998) World reference base for soil resources. Food and Agriculture Organization of the United Nations, Rome

Forsythe WC, Rykiel EJ Jr, Stahl RS, Wu H, Schoolfield RM (1995) A model comparison for daylength as a function of latitude and day of year. Ecol Modell 80:87–95

Fritts HC (1976) Tree rings and climate. Academic Press, London

Gärtner H, Nievergelt D (2010) The core-microtome: a new tool for surface preparation on cores and time series analysis of varying cell parameters. Dendrochronologia 28:85–92

Gensler GA (1946) Der Begriff der Vegetationszeit. Dissertation, Universität Zürich, Engadin Press, Samedan

Godet J-D (1986) Bäume und Sträucher: einheimische und eingeführte Baum- und Straucharten. Arboris-Verlag, Hinterkappelen-Bern

Hall DB, Clutter M (2004) Multivariate multilevel nonlinear mixed effects models for timber yield predictions. Biometrics 60:16–24

Heiri C, Wolf A, Rohrer L, Bugmann H (2009) Forty years of natural dynamics in Swiss beech forests: structure, composition, and the influence of former management. Ecol Appl 19:1920–1934

Holmes RL (1983) Computer-assisted quality control in tree-ring dating and measurement. Tree-Ring Bull 43:69–78

Johnson JB, Omland KS (2004) Model selection in ecology and evolution. Trends Ecol Evol 19:101–108

Kleinschmit J, Kleinschmit JGR (2000) *Quercus robur–Quercus petraea*: a critical review of the species concept. Glasnik Za Smske Pokuse 37:441–452

Lappi J, Bailey RL (1988) A height prediction model with random stand and tree parameters: an alternative to traditional site index methods. For Sci 34:907–927

Martin-Benito D, Kint V, del Río M, Muys B, Cañellas I (2011) Growth responses of West-Mediterranean *Pinus nigra* to climate

change are modulated by competition and productivity: past trends and future perspectives. For Ecol Manag 262:1030–1040

Muir G, Fleming CC, Schlötterer C (2000) Species status of hybridizing oaks. Nature 405:1016

Nothdurft A, Kublin E, Lappi J (2006) A non-linear hierarchical mixed model to describe tree height growth. Eur J For Res 125:281–289

Parker GR, Leopold DJ (1983) Replacement of *Ulmus americana* L. in a mature east-central Indiana woods. Bull Torrey Bot Club 110:482–488

Piedallu C, Gégout J-C, Bruand A, Seynave I (2011) Mapping soil water holding capacity over large areas to predict potential production of forest stands. Geoderma 160:355–366

Pinheiro JC, Bates DM (2000) Mixed-effects models in S and S-PLUS. Statistics and Computing, Springer, New York

Pinheiro J, Bates D, DebRoy S, Sarkar D, R Development Core Team (2011) nlme: linear and nonlinear mixed effects models. R package version 3.1-104

Ranius T, Jansson N (2000) The influence of forest regrowth, original canopy cover and tree size on saproxylic beetles associated with old oaks. Biol Conserv 95:85–94

R Development Core Team (2010) R: a language and environment for statistical computing. R Foundation for Statistical Computing. Vienna, http://www.R-project.org

Richards FJ (1959) A flexible growth function for empirical use. J Exp Bot 10:290–300

Rohner B (2012) Growth and mortality of oak (*Quercus* spp.): a combined analysis of monitoring and tree-ring data from Swiss forest reserves. Dissertation, ETH Zurich, Zurich

Rohner B, Bigler C, Wunder J, Brang P, Bugmann H (2012) Fifty years of natural succession in Swiss forest reserves: changes in stand structure and mortality rates of oak and beech. J Veg Sci 23:892–905

Rohner B, Bugmann H, Bigler C (2013) Towards non-destructive estimation of tree age. For Ecol Manage 304:286–295

Rozas V (2003) Tree age estimates in *Fagus sylvatica* and *Quercus robur*: testing previous and improved methods. Plant Ecol 167:193–212

Rozas V (2005) Dendrochronology of pedunculate oak (*Quercus robur* L.) in an old-growth pollarded woodland in northern Spain: establishment patterns and the management history. Ann For Sci 62:13–22

Russell MB, Weiskittel AR, Kershaw JA Jr (2011) Assessing model performance in forecasting long-term individual tree diameter versus basal area increment for the primary Acadian tree species. Can J For Res 41:2267–2275

Subedi N, Sharma M (2011) Individual-tree diameter growth models for black spruce and jack pine plantations in northern Ontario. For Ecol Manage 261:2140–2148

Tesch SD (1981) The evolution of forest yield determination and site classification. For Ecol Manage 3:169–182

Thornthwaite CW (1948) An approach toward a rational classification of climate. Geogr Rev 38:55–94

Thornton PE, Running SW, White MA (1997) Generating surfaces of daily meteorological variables over large regions of complex terrain. J Hydrol 190:214–251

von Bertalanffy L (1957) Quantitative laws in metabolism and growth. Q Rev Biol 32:217–231

Weber P, Bugmann H, Rigling A (2007) Radial growth responses to drought of *Pinus sylvestris* and *Quercus pubescens* in an inner-Alpine dry valley. J Veg Sci 18:777–792

Weber P, Bugmann H, Fonti P, Rigling A (2008) Using a retrospective dynamic competition index to reconstruct forest succession. For Ecol Manage 254:96–106

Weiskittel AR, Hann DW, Kershaw JA Jr, Vanclay JK (2011) Forest growth and yield modeling. Wiley-Blackwell, Chichester

Willmott CJ, Rowe CM, Mintz Y (1985) Climatology of the terrestrial seasonal water cycle. J Climatol 5:589–606

Zeide B (1993) Analysis of growth equations. For Sci 39:594–616